Original Article
Synergistic protection of tetramethylpyrazine phosphate and borneol on brain microvascular endothelium cells injured by hypoxia

Bin Yu[1], Fen-Miao Zhong[2], Yao Yao[1], Shuo-Qiu Deng[1], Hui-Qin Xu[1], Jin-Fu Lu[1], Ming Ruan[1,3], Xiang-Chun Shen[4]

[1]Jiangsu Key Laboratory for Pharmacology and Safety Evaluation of Chinese Materia Medica, School of Pharmacy, Nanjing University of Chinese Medicine, Nanjing 210023, China; [2]Nanjing Foreign Language School, Nanjing 210008, China; [3]Jiangsu Provincial Key Construction Laboratory of Special Biomass Waste Resource Utilization, School of Food Science, Nanjing Xiaozhuang University, Nanjing 211117, China; [4]The Key Laboratory of Optimal Utilization of Natural Medicinal Resources, School of Pharmaceutic Science, Guizhou Medical University, Guiyang 550025, China

Abstract: The combination of tetramethylpyrazine phosphate (TMPP) and borneol (BO) protects against cerebral ischemia. However, the mechanism for their synergistic effect is unclear. In this study, an oxygen-glucose deprivation (OGD) injured brain model was induced in microvascular endothelium cells (BMECs). TMPP and BO concentrations were optimized according to an MTT assay. Cells were divided into five groups: control, model, TMPP, BO, and TMPP+BO. Subsequently, oxidative stress was evaluated based on the levels of superoxide dismutase (SOD), malondialdehyde (MDA), catalase (CAT), glutathione peroxidase (GSH-Px), and reactive oxygen species (ROS). Intracellular calcium ($[Ca^{2+}]i$) was detected using a laser confocal microscope. Cellular apoptosis was examined via Hoechst 33342 staining, flow cytometry, and expression of p53, B-cell lymphoma 2 (BCL-2), BCL-2-like protein 4 (BAX), and caspase-3 mRNA. Angiogenesis was evaluated based on expression of basic fibroblast growth factor (bFGF), vascular endothelial growth factor (VEGF), fibroblast growth factor receptor 1 (FGFR1), Vascular endothelial growth factor receptor 1 (VEGFR1), and VEGFR2. Results showed that 5.0 µM TMPP and 0.5 µM BO were optimal. Monotherapy significantly enhanced CAT, BCL-2, and VEGF, and also reduced $[Ca^{2+}]i$, apoptosis, and BAX. TMPP increased SOD, GSH-Px, and bFGF, and reduced MDA, ROS, p53, and caspase-3 levels. BO reduced VEGFR1 expression. TMPP+BO combination exhibited synergistic effects in decreasing apoptosis, and modulating expression of BCL-2, BAX, and VEGFR1. These results indicate that protection of OGD-injured BMECs by TMPP+BO combination involves anti-oxidation, apoptosis inhibition, and angiogenesis. Moreover, their synergistic mechanism was mainly related to the regulation of apoptosis and angiogenesis.

Keywords: Synergistic effect, tetramethylpyrazine phosphate, borneol, BMECs, apoptosis, angiogenesis

Introduction

Ischemic stroke, the third leading cause of human death, has a very complex pathophysiological mechanism involving neuronal and cerebrovascular damage. Apart from neuroprotection, maintenance of an intact vascular system and induction of angiogenesis for delivery of oxygen and nutrients are important in reducing damage [1]. Presently the routine treatment in the clinic for stroke includes eliminating thrombus and improving blood circulation in brain tissue. Increasing evidence suggests that survival and regeneration of brain microvascular endothelium cells (BMECs) can reduce neuronal damage caused by ischemic attack via remodeling injured tissue, generating new blood vessels, and inducing neurogenesis [2]. Therefore, drugs targeting the activation of BMECs are needed for neuronal repair therapy.

Tetramethylpyrazine (TMP) is one of the most effective ingredients from *Ligusticum chuanxiong Hort* (chuanxiong), which has been used as a traditional Chinese medicinal herb for thousands of years. TMP phosphate (TMPP), a

commercial product, is usually prescribed to patients with brain ischemia in the clinic. Studies have found that TMPP protects the cerebral vasculature from ischemic injury by promoting endothelial cell survival, reducing oxidative stress [3], inhibiting the cascade reaction of apoptosis [4] and increasing proliferation [5]. Borneol (BO), a resin from *Dryobalanops aromatica Gaertn. F.*, is another traditional Chinese medicine. BO attenuates Alzheimer's disease, stroke, cerebral ischemia, cerebritis, and cerebral edema [6]. Studies have found that BO protects against cerebral ischemic injury by inhibiting oxidation and apoptosis and maintaining blood-brain barrier (BBB) stability [7-9]. According to traditional Chinese medicine theory, BO can also direct drugs upward to the head targeting the brain. Our previous research suggested that BO helped other drugs to efficiently cross the BBB and distribute in the brain [10, 11]. Subsequently, BOs ability to open the BBB was accepted by other scholars [12]. Interestingly, TMPP is just one of BOs substrates [13]. Our previous studies have confirmed the synergistic neuroprotection of TMPP and BO against ischemia attack in the cortex, hippocampus, hypothalamus, and striatum via regulating apoptosis and autophagy [14-16].

BMEC protection is an effective method to attenuate brain ischemia. However, the mechanism for the synergistic effect of TMPP and BO is still unclear. The present study investigated their mechanism of protection for BMECs against oxygen-glucose deprivation (OGD) injury, and especially their effect on oxidative stress, $[Ca^{2+}]i$, apoptosis, and regeneration. Additionally, the synergy of TMPP and BO was investigated to further understand their clinical application.

Materials and methods

Culture of primary BMECs

BMECs were obtained from 24-h-old neonatal Sprague Dawley (SD) rats as described previously [17, 18]. Briefly, male and female neonatal rats were anesthetized with isoflurane and killed by cervical dislocation. The forebrain was removed, and brainstems, cerebella, thalami, and blood vessels were isolated. The remaining tissue was cut into 1-mm³ sections by eye and homogenized in DMEM/F12 at 4°C. The homogenate was centrifuged and re-suspended in DMEM/F12. The suspension was filtered through a 20-μm nylon screen mesh. BMECs retained on the screen mesh were collected and digested with type-2 collagenase. After digestion, the precipitate was suspended in 20% bovine serum albumin (BSA) and centrifuged. After centrifugation, pellets were re-suspended and washed again. Then BMECs were collected and seeded into a 75-cm³ culture flask coated with gelatin. The cells were cultured in DMEM medium supplemented with 20% fetal bovine serum, 1% penicillin-streptomycin, 80 μg/mL heparin, 2 mM glutamine, and 75 μg/mL endothelial cell growth supplement. They were maintained in a 37°C incubator with 5% CO_2 and 95% air. When the BMECs were 90% confluent, they were used in the following experiments.

This study was approved by the Animal Ethics Committee of Nanjing University of Chinese Medicine, and the experiments were performed according to the guidelines of laboratory animal care (Institute of Laboratory Animal Resources, Commission on Life Sciences, National Research Council, 1996).

OGD in vitro model

BMECs were subjected to OGD injury as previously described [2]. Briefly, culture media was replaced with glucose-free DMEM, perfused with 5% CO_2 and 95% N_2 gas to induce hypoxia for 4 h at 37°C, and then cultured normally for 12 h to imitate reperfusion injury.

Identification of BMECs

Typical cobblestone morphology and expression of factor VIII-associated antigen are the characteristic features of BMECs. To identify BMECs in the present study, the expression of factor VIII-associated antigen was measured by immunocytochemistry, as described previously [19, 20]. BMECs ($1×10^4$) were seeded on a 24-well plate coated with gelatin with a coverslip on the bottom. Cells were washed with PBS, fixed with 4% formaldehyde for 20 min, and then incubated with 0.1% Triton X-100 for 15 min and 3% H_2O_2 for 30 min successively. Then 10% BSA was used to block non-specific binding on the cells at room temperature. BMECs were incubated with primary antibody against factor VIII-associated antigen (1:1000; Cell Signaling Technology, Beverly, MA, USA) overnight at 4°C. Then the cells were incubated

with HRP-conjugated secondary antibody (1:500, Wuhan Boster Biological Technology, China) for 30 min at 37°C. Cells were stained with 3,3'-Diaminobenzidine (DAB) for 3 min and co-stained with hematoxylin. Then the slides were mounted with triglyceride and analyzed with a microscope. The cytoplasm of positive cells was brown.

Dose optimization of TMPP and BO using MTT assay

The MTT assay is an indirect measurement of cell viability. Living cells transform MTT into formazan using mitochondrial succinate dehydrogenase. BMECs ($3×10^3$/well) were seeded in a 96-well plate and divided into 10 groups including control, model, TMPP groups (0.05, 0.5, 5, and 50 µM), and BO groups (0.05, 0.5, 5 and 50 µM). Both the control and model group were incubated with DMSO. The other eight groups were incubated with the specified concentrations of TMPP or BO. After 4 h of OGD and 12 h of reperfusion, BMECs were mixed with MTT to produce a 1.2 mM concentration per well. Then the cells were continuously incubated for 1.5 h at 37°C. Following this, the culture medium was removed, the precipitant was solubilized in DMSO, and absorbance was detected at a wavelength of 490 nm using a Synergy-HT microplate reader (Bio-Tek Instruments, USA).

Relative survival rate (%) = (experiment group absorbance/control group absorbance) ×100

The optimized doses of TMPP and BO were obtained from the MTT assay results and used in the following studies. The TMPP+BO group was treated with the combination of their optimized doses. Control and model groups were treated with DMSO, while the control group did not receive OGD injury. Cells were exposed to drugs throughout the whole period of OGD and reperfusion. After reperfusion, the cells were used for the following assays.

Antioxidant measurements

The concentration of superoxide dismutase (SOD), malondialdehyde (MDA), catalase (CAT), and glutathione peroxidase (GSH-Px) in culture medium was measured with a colorimetric assay according to the manufacturer's protocol (Nanjing Jiancheng Bioengineering Institute,

Nanjing, China). The level of intracellular reactive oxygen species (ROS) was measured by the conversion of non-fluorescent DCFH-DA to its fluorescent derivative. After BMECs were washed with cold PBS, fluorescence intensity was measured at 535 nm with a Synergy-HT microplate reader according to the manufacturer's protocol (Nanjing Jiancheng Bioengineering Institute, Nanjing, China).

Laser confocal Ca^{2+} imaging

When BMECs reached 90% confluence on a 24-well plate coated with gelatin with a coverslip on the bottom, they were exposed to OGD/reperfusion injury and the corresponding drugs. They were then incubated with 5 µM Fluo-3/AM (Biotium, Hayward, CA, USA) for 30 min, and washed twice with PBS. The fluorescence intensities of BMECs were detected using a laser scanning confocal microscope (Leica TCS-SP5, Solms, Germany). Line scanning mode was used at a scan rate of 1 kHz. The excitation wavelength was 488 nm, and the emission wavelength was 505-530 nm. Fluorescence intensity reflected the intracellular calcium content.

Hoechst 33342 staining for apoptosis

Culture medium was removed, and cells were washed with PBS twice. Then 200 µL 4% paraformaldehyde was added to each well to fix cells for 20 min, followed by four washes with PBS. Hoechst 33342 (100 µL) staining reagent was added to each well and kept at 37°C for 20 min. Cells were then rinsed with PBS four times and observed under an inverted fluorescence microscope (IX71, Olympus, Japan). The excitation wavelength was 346 nm, and the emission wavelength was 460 nm. Apoptotic nuclei were densely stained blue. The average number of positive nuclei and the total nuclei were counted from three random visual fields. Apoptosis (%) was calculated as the ratio of positive nuclei to total nuclei.

Flow cytometry for apoptosis

BMECs were disassociated with trypsin, washed with PBS, counted, and transferred to a reaction tube at a density of $5×10^4$/mL. Cells were then incubated with Annexin V FITC and propidium iodide (PI) staining reagent. Apoptosis (%) was measured using a flow cytometer (Cytomics FC 500 MPL, Beckman Coulter, USA) according to the manufacturer's protocol.

Table 1. The accession numbers, primers of proteins and sizes in real-time PCR assay

Target genes	Accession no.	Forward (5'-3')	Reverse (5'-3')	Size (bp)
Bcl-2	DQ926871.1	GAGATGTCCAGCCAGCTG	TAGGCACCCAGGGTGATG	365
Bax	DQ926869.1	CAGCTCTGAGCAGATCATG	TGGTGGCCTCAGCCCATCT	539
P53	NM_205264.1	GAGTGCTGAAGGAGATCAATGAG	GTGGTCAGTCCGAGCCTTTT	145
Caspase-3	NM_001009338.1	GTGTGCGTTAGAAGTACC	GTTCTTTTGTGAGCATAG ACA	834
GAPDH	NM_017008.4	GTTCAACGGCACAGTCAAG	GCCAGTAGACTCCACGACAT	136

Real-time PCR

Total RNA was extracted from cells using Trizol reagent according to the manufacturer's protocol. RNA was reverse transcribed using an iScript cDNA Synthesis Kit (Bio-Rad, Hercules, CA, USA). BCL-2, BAX, p53, caspase-3, and GAPDH cDNA were amplified by real-time PCR using the SYBR Premix Ex Taq kit (TakaRa Bio Inc., Shiga, Japan) in an MJ Mini thermal cycler (Bio-Rad). The amplification was performed under the following conditions: pre-incubation at 95°C for 5 min followed by 40 cycles of 95°C for 15 s and 60°C for 40 s. Melting curve analysis was performed from 55-95°C. Cycle number threshold (Ct) of each reaction was calculated from the amplification curve using the $2^{-\Delta\Delta Ct}$ method to derive relative gene expression. GAPDH served as an internal control. Accession numbers, primers, and product sizes are shown in **Table 1**.

Western blot for angiogenesis

BMECs were harvested and lysed in cold RIPA Lysis Buffer (Thermo Scientific, Inc. USA) on ice. The lysate was centrifuged at 12,000 rpm for 15 min at 4°C. Part of the supernatant was used to determine the protein concentration using a BCA protein assay kit (Nanjing KeyGen Biotech. Co., Ltd., Nanjing, China). The rest of the supernatant was diluted to 7 μg/μL with gel loading buffer and heated for 5 min at 95°C. Then, 10 μL (70 μg) of protein sample was separated by SDS-PAGE and transferred to a poly-vinylidene fluoride (PVDF) membrane. The membrane was blocked for 2 h at room temperature in Tris-buffered saline with Tween-20 (TBST) containing 5% BSA. The membrane was then probed with the following primary antibodies overnight at 4°C: anti-bFGF (1:1000; Santa Cruz Biotechnologies, Dallas, TX, USA), anti-FGFR1 and anti-VEGF (Proteintech Group, Inc, Rosemont, USA), and anti-VEGFR1 and VEGFR2 (1:1000; Abcam, Cambridge, UK). Anti-β-actin

(1:5000; Bioworld Technology, Inc., St. Louis Park, MN, USA) was used as a control for protein loading. After washing in TBST, the membrane was incubated for 2 h with secondary antibody (goat anti-rabbit or rabbit anti-mouse 1:10,000, Boster Biotechnology, Ltd., Wuhan, China). Protein was detected by enhanced chemiluminescence, and blots were analyzed using Image-J software. β-actin was used for normalization.

Statistical analysis

All data were expressed as mean ± standard deviation (SD) and analyzed using SPSS 13.0 software. Statistical differences between groups were analyzed by one-way analysis of variance (ANOVA) and Tukey's multiple comparison post hoc tests. A *p*-value less than 0.05 was considered statistically significant.

Results

Identification of BMECs

As shown in **Figure 1A**, the morphology of BMECs under a microscope was a typical cobblestone pattern, which is regarded as a characteristic feature of BMECs. Moreover, brown cytoplasm denoted positive expression of factor VIII-associated antigen, which is regarded as an immunological characteristic of BMECs, as shown in **Figure 1B**. The purity of BMECs was over 90%.

Dose optimization of TMPP and BO using MTT assay

As shown in **Figure 2**, the relative survival rate of BMECs in the model group decreased significantly as compared to the control group (P< 0.01), which indicates that OGD caused severe damage to the cells. However, both TMPP (0.5, 5.0, and 50 μM) and BO (0.5 and 5.0 μM) displayed significant protection from OGD injury in the cells. Additionally, they showed a concen-
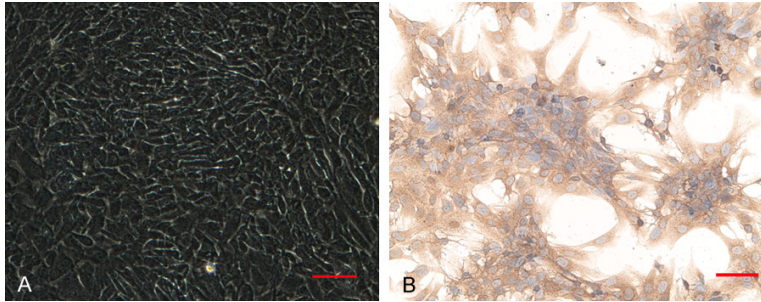
Figure 1. Identification of BMECs. A. Representative photograph of BMECs under a microscope. The cells had a typical cobblestone morphology. B. Representative photograph of BMECs using immunocytochemistry. Brown cytoplasm denotes positive expression of factor VIII-associated antigen, an immunological characteristic of BMECs. Scale bar represents 50 μm.
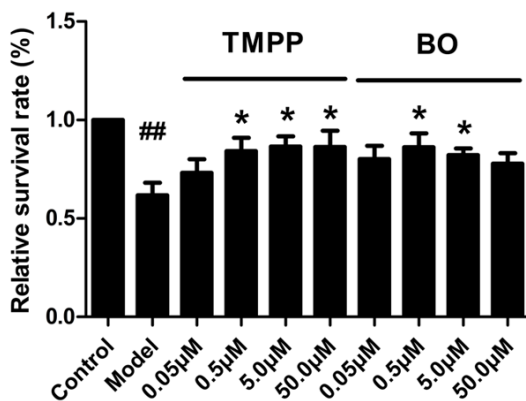

Figure 2. Optimization of TMPP and BO concentration for BMEC survival after OGD injury (n=6). TMPP at 0.5, 5.0, and 50 μM increased the survival of OGD-injured BMECs and 5.0 μM TMPP showed the best protection among those concentrations. Meanwhile, 0.5 and 5.0 μM BO had a similar protective effect on BMECs, and its most effective concentration was 0.5 μM. These two optimal concentrations (5.0 μM TMPP and 0.5 μM BO) were used in the following experiments.

tration-dependent protection up until 5.0 μM TMPP and 0.5 μM BO. Therefore, 5.0 μM TMPP and 0.5 μM BO were regarded as the optimized doses and used in the following studies.

Cooperative effect of TMPP and BO on antioxidant induction

TMPP and BO had a synergistic effect on antioxidant induction as displayed in **Figure 3**. OGD injury markedly reduced the activity of SOD, CAT, and GSH-Px, and increased the concentration of MDA and ROS (P<0.01), which is indicative of oxidative stress. Besides reducing MDA and ROS (P<0.01), 5.0 μM TMPP could enhance SOD, CAT, and GSH-Px levels (P<0.05). However,

BO only enhanced CAT (P< 0.05). TMPP+BO combination displayed a stronger therapeutic effect on MDA (P< 0.05) and ROS (P<0.01) than monotherapy of BO. But, TMPP+BO did not show any further improvement than the TMPP monotherapy group (P> 0.05).

TMPP and BO cooperatively regulate [Ca²⁺]i

The synergistic effect of TMPP+BO on [Ca²⁺]i modulation is shown in **Figure 4**. Compared to the control group, the model group significantly increased [Ca²⁺]i (P<0.01), which is suggestive of Ca²⁺ overload. Treatment with TMPP, BO, and their combination attenuated [Ca²⁺]i (P<0.01 or P< 0.05). However, TMPP+BO combination did not shower further improvement than monotherapy (P>0.05). These results indicate that TMPP+ BO did not have a synergistic effect on Ca²⁺ overload relief.

TMPP and BO cooperatively reduce apoptosis

Figure 5A and **5B** illustrate the results of the Hoechst 33342 staining. Cellular apoptosis can induce nuclei to turn densely blue in this assay. Compared to the control group, the model group significantly increased apoptosis (P<0.01), which suggests that OGD injury induces apoptosis. Both 5.0 μM TMPP and 0.5 μM BO reduced apoptosis (P<0.05). Moreover, TMPP+BO treatment had a synergistic effect exhibiting greater improvement than monotherapy treatment (P<0.05), which indicates the advantage of their combination in preventing apoptosis.

Figure 5C and **5D** illustrate the results of flow cytometry which were similar to that of the Hoechst 33342 staining. Compared to the control group, OGD injury induced an abrupt increase in apoptosis (P<0.01). However, both 5.0 μM TMPP and 0.5 μM BO reversed the apoptosis (P<0.01). Similarly, TMPP+BO combination therapy exhibited greater protection against apoptosis than monotherapy treatment (P<0.01), which highlights the advantage of their combination in preventing apoptosis.
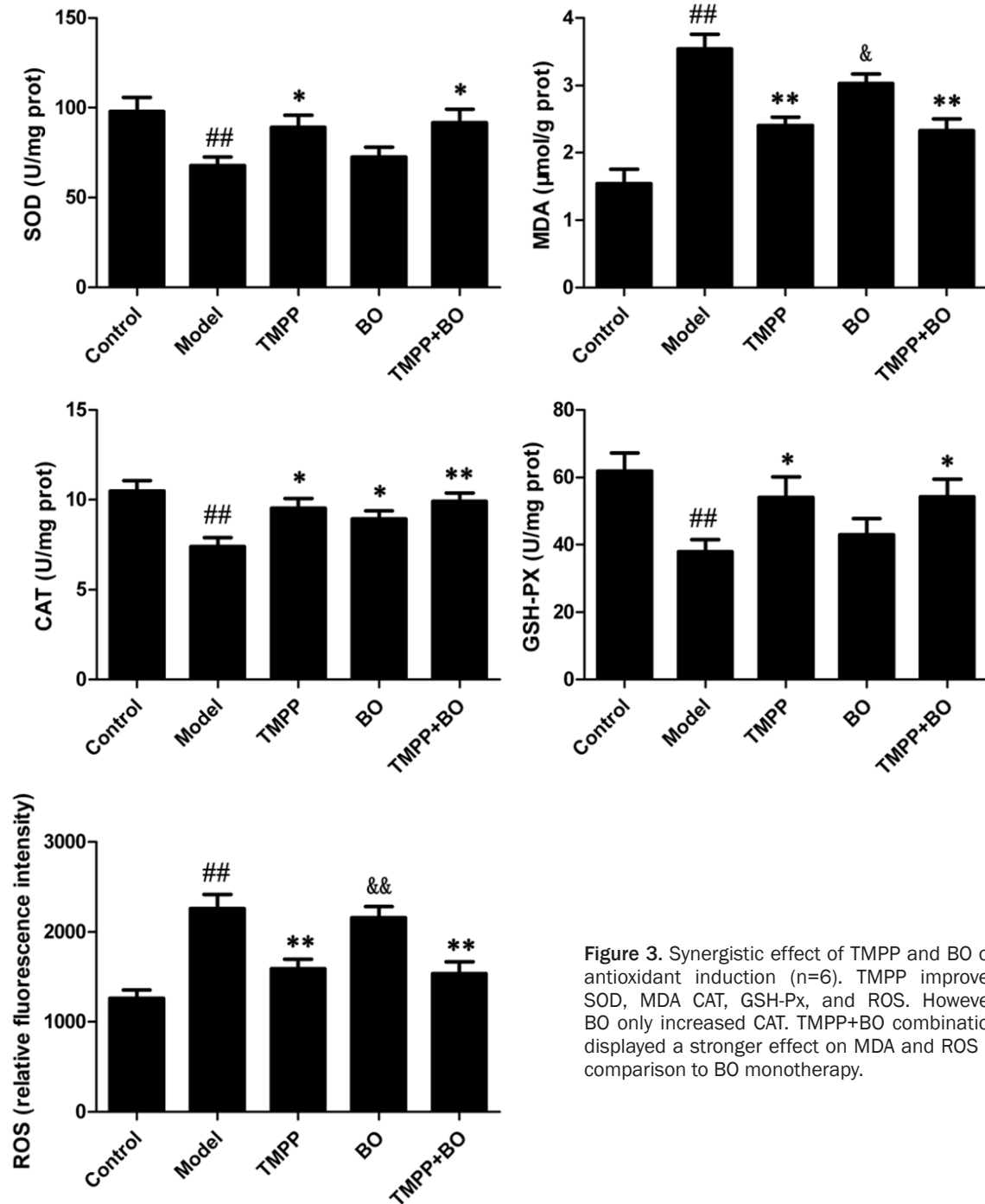
Figure 3. Synergistic effect of TMPP and BO on antioxidant induction (n=6). TMPP improved SOD, MDA CAT, GSH-Px, and ROS. However, BO only increased CAT. TMPP+BO combination displayed a stronger effect on MDA and ROS in comparison to BO monotherapy.

TMPP and BO cooperatively regulate the expression of BCL-2, BAX, p53, and caspase-3 mRNA

As shown in **Figure 6**, expression of BAX, p53, and caspase-3 mRNA was markedly upregulated (P<0.05) while BCL-2 was downregulated (P<0.01) in the model group compared to the control group. Similar to the above results from the Hoechst 33342 staining and flow cytometry this suggests that apoptosis was induced by OGD injury. Both 5.0 μM TMPP and 0.5 μM BO upregulated the expression of BCL-2 and down-regulated that of BAX (P<0.05). Additionally, TMPP reduced the expression of p53 and cas-pase-3 (P<0.05). Compared to the model group, the combination group increased the level of BCL-2 (P<0.05) and decreased the level of BAX,
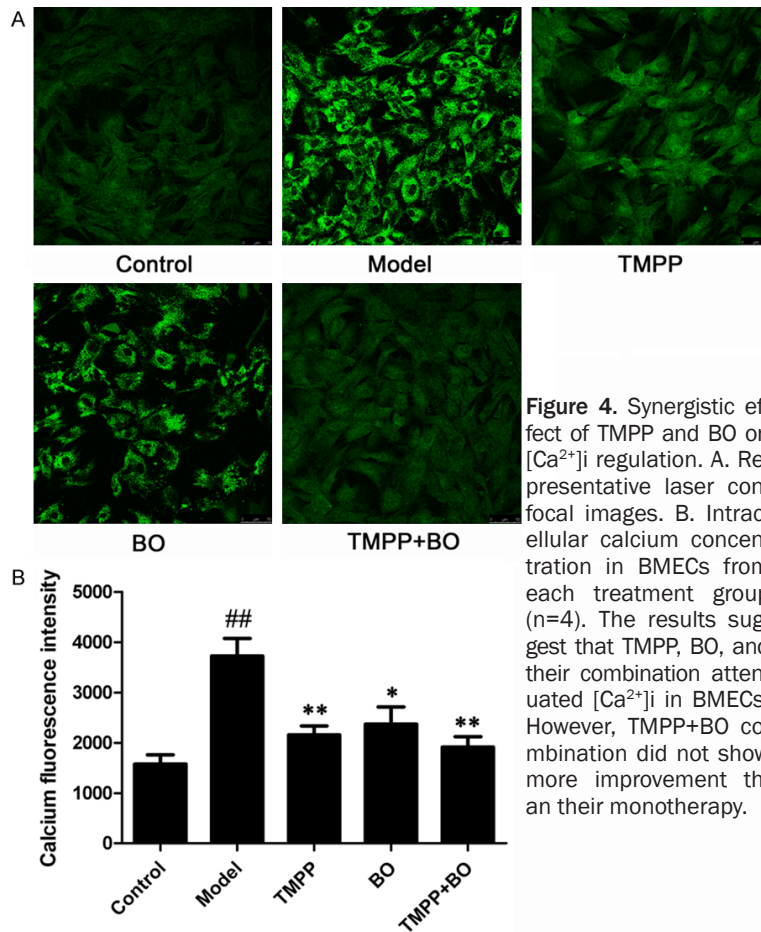
Figure 4. Synergistic effect of TMPP and BO on $[Ca^{2+}]i$ regulation. A. Representative laser confocal images. B. Intracellular calcium concentration in BMECs from each treatment group (n=4). The results suggest that TMPP, BO, and their combination attenuated $[Ca^{2+}]i$ in BMECs. However, TMPP+BO combination did not show more improvement than their monotherapy.

and VEGF (P<0.05 and P< 0.01, respectively), while BO enhanced VEGF and suppressed VEGFR1 (P<0.05). TMPP+BO combination significantly modulated bFGF (P<0.05), VEGF (P<0.01), and VEGFR1 (P<0.01). Furthermore, the combination group more significantly reduced VEGFR1 expression than monotherapy groups (P<0.05 vs. P<0.01).

Discussion

Recently, a large-scale survey of 480,687 adults reported that the prevalence of stroke was 1.114%, and cerebral ischemic stroke accounted for 69.6% [22]. Therefore, the development of a new drug or improvement of existing drugs for stroke with a clear mechanism has drawn the attention of cerebrovascular disease scholars all over the world.

TMPP, as a commercial medicine, relieves stroke damage in the clinic. BO has also been prescribed for central nervous system (CNS) diseases including cerebral ischemia, for thousands of years. In addition, their combination is usually employed for a better therapeutic effect on stroke treatment. However, their synergistic mechanism was not understood until now. Our previous studies suggest that the combined treatment has a stronger therapeutic effect than any of the drugs alone, and part of its mechanism involves neuroprotection, including decreasing oxidative stress, preventing neuron loss, and anti-inflammatory activities [14]. Further, we discovered that their synergistic protection was also related to modulation of apoptosis and autophagy [15, 16]. Although many neuroprotective monotherapy drugs have been shown to attenuate the ischemic cascade in preclinical models, their clinical trials failed to show efficacy even in early cascade events of ischemic stroke [23, 24]. Considering this disaccord, the importance of protecting BMECs, improving their function, and inducing angiogenesis in ischemic areas have

p53, and caspase-3 (P<0.01). Additionally, compared to the TMPP group, the model group exhibited stronger effects in modulating the levels of BCL-2 and BAX (P<0.05). Compared to the BO group, the model group also more strongly regulated gene expression (P<0.05). These results might explain its advantage in reducing BMEC apoptosis, as shown in **Figure 5**.

TMPP and BO cooperatively regulate the expression of angiogenesis-related proteins

Figure 7 displays the cooperative effect of TMPP+BO on the regulation of angiogenesis-related protein expression. Compared to the control group, the model group increased the expression of FGFR1 and VEGFR1 (P<0.01 and P<0.05, respectively), which indicates that OGD injury induced angiogenesis as previously reported [21]. Interestingly, 5.0 µM TMPP and 0.5 µM BO further promoted angiogenesis while having different angiogenesis targets. Specifically, TMPP enhanced the expression of bFGF
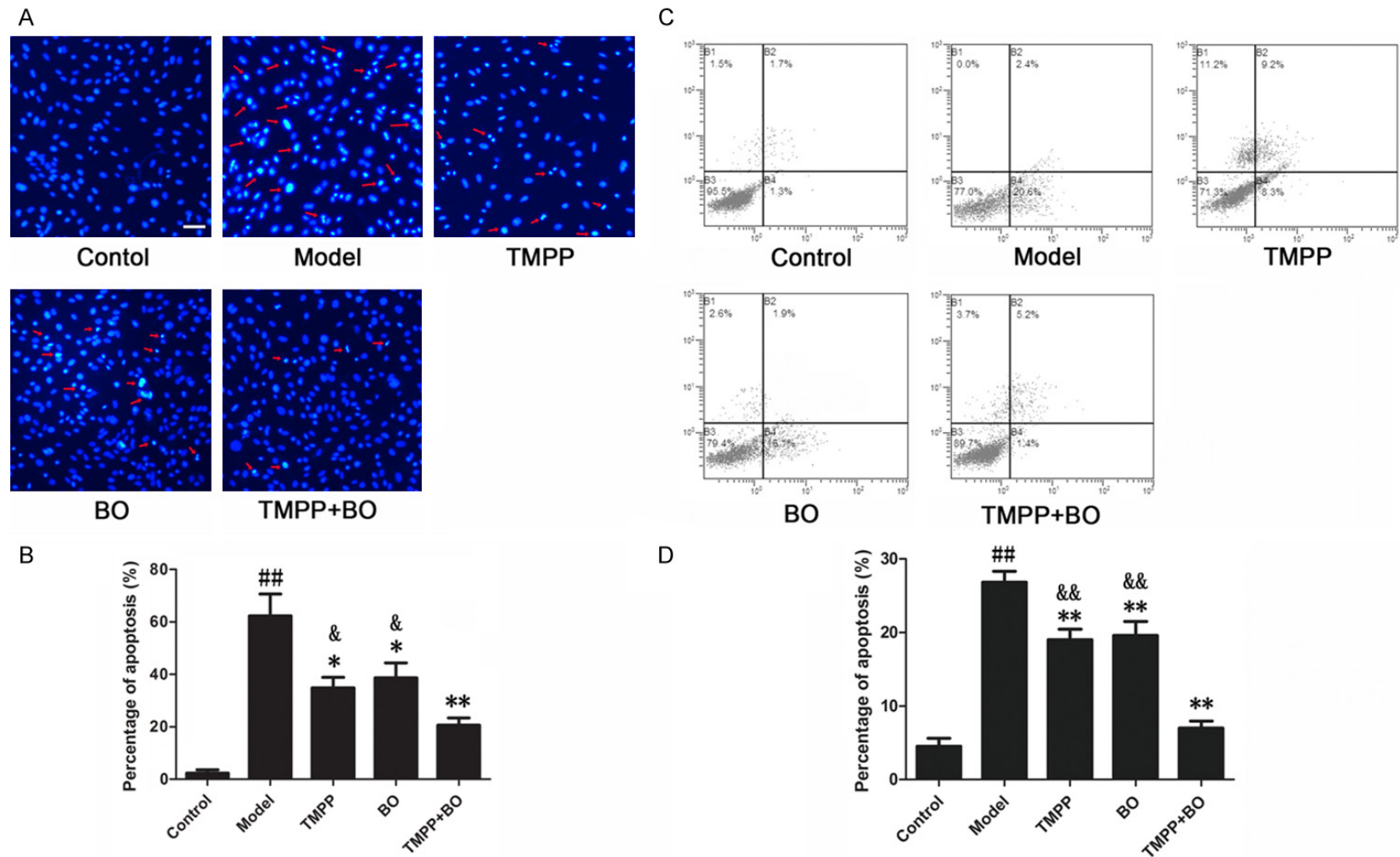
Figure 5. Synergistic effect of TMPP and BO on reducing apoptosis. A. Representative images of Hoechst 33342 staining assay. Apoptotic cells are marked with red arrows. B. Percentage of BMECs undergoing apoptosis as measured by Hoechst 33342 staining assay (n=6). C. Representative flow cytometry images. D. Percentage of BMECs undergoing apoptosis as measured by flow cytometry (n=6). Results from both assays were similar demonstrating that TMPP, BO, and TMPP+BO combination significantly decreased apoptosis. TMPP+BO combination displayed a synergistic effect showing greater protection than monotherapy. Scale bar represents 50 μm.
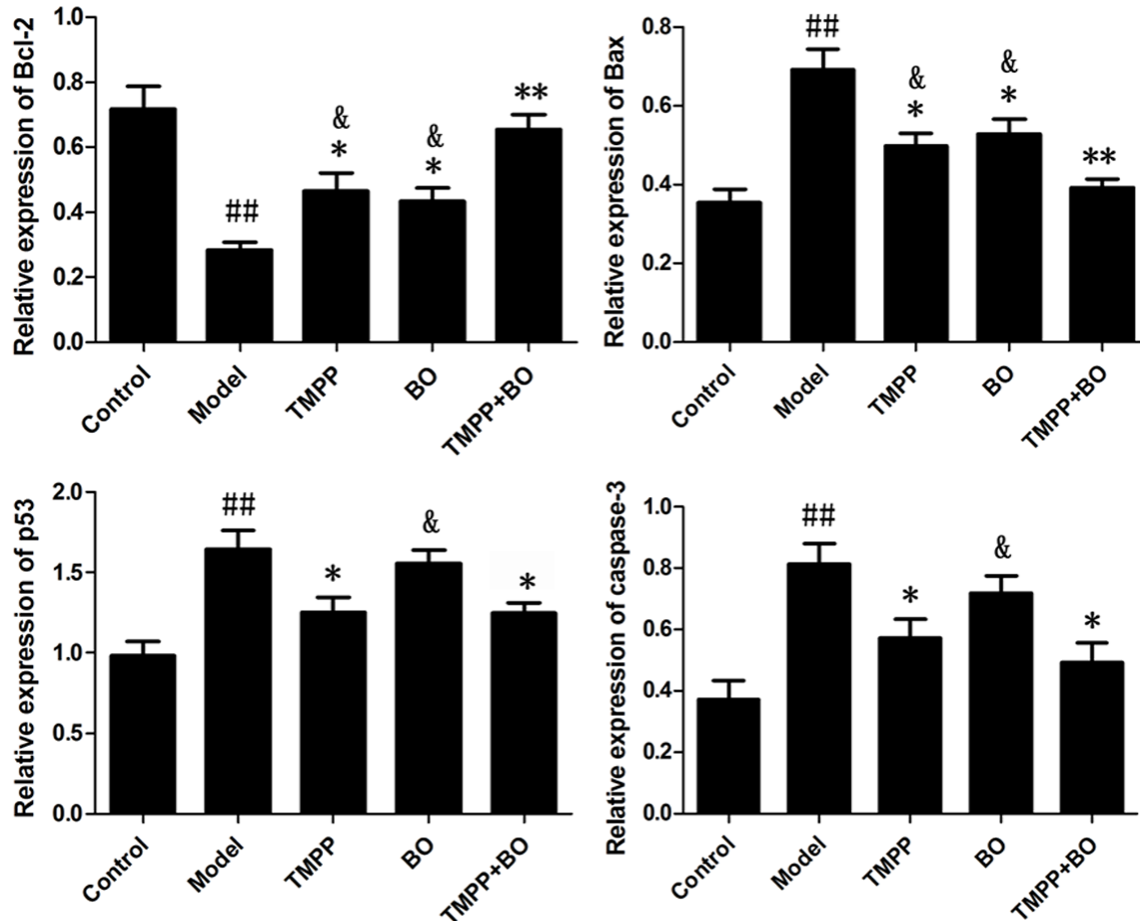
Figure 6. Synergistic effect of TMPP and BO on regulating the expression of BCL-2, BAX, p53, and caspase-3 mRNA (n=4). Results indicate that the anti-apoptosis effect of TMPP was involved in modulating the expression of BCL-2, BAX, p53, and caspase-3 mRNA, while BO was involved in modulating BCL-2 and BAX mRNA. Additionally, TMPP+BO combination exhibited more significant modulation than monotherapy.

been realized. The present study was proposed based on these findings.

It is well known that mitochondria are very sensitive to hypoxia. When ischemia damages brain tissue, the mitochondria in BMECs enhance oxidative stress by decreasing SOD, CAT and GSH-Px activity, and increasing ROS and MDA levels [25]. In the present study, OGD imitated the damage caused by cerebrovascular ischemia-reperfusion injury. The results suggest that 5.0 μM TMPP enhanced the activity of SOD, CAT, and GSH-Px, and reduced levels of MDA and ROS in OGD-injured BMECs. Additionally, 0.5 μM BO increased CAT activity. Moreover, the TMPP+BO combination showed greater improvement of MDA and ROS levels than monotherapy of BO.

Excessive oxidative stress often leads to cell membrane deficiency, triggers excessive Ca²⁺

influx, and even induces Ca²⁺ overload. Ca²⁺ overload contributes to the detrimental cascade of ischemic injury and is regarded as another important injury factor. Additionally, Ca²⁺ overload exacerbates oxidative damage. Thus, a vicious circle is formed [26]. In the present study, TMPP, BO, and TMPP+BO combination attenuated [Ca²⁺]i in BMECs suffering from OGD damage. Interestingly, TMPP+BO combination was not more effective than monotherapy indicating that their modulation on [Ca²⁺]i might be indirect.

Hypoxia causes BMECs to undergo apoptosis [27]. The mechanism is closely related to Ca²⁺ overload because Ca²⁺ activates the caspase-3 pathway. Caspase-3 is the main terminal peptidase in apoptosis and plays a critical role. Removal of caspase-3 from cell extracts inhibits apoptosis, while the addition of exogenous
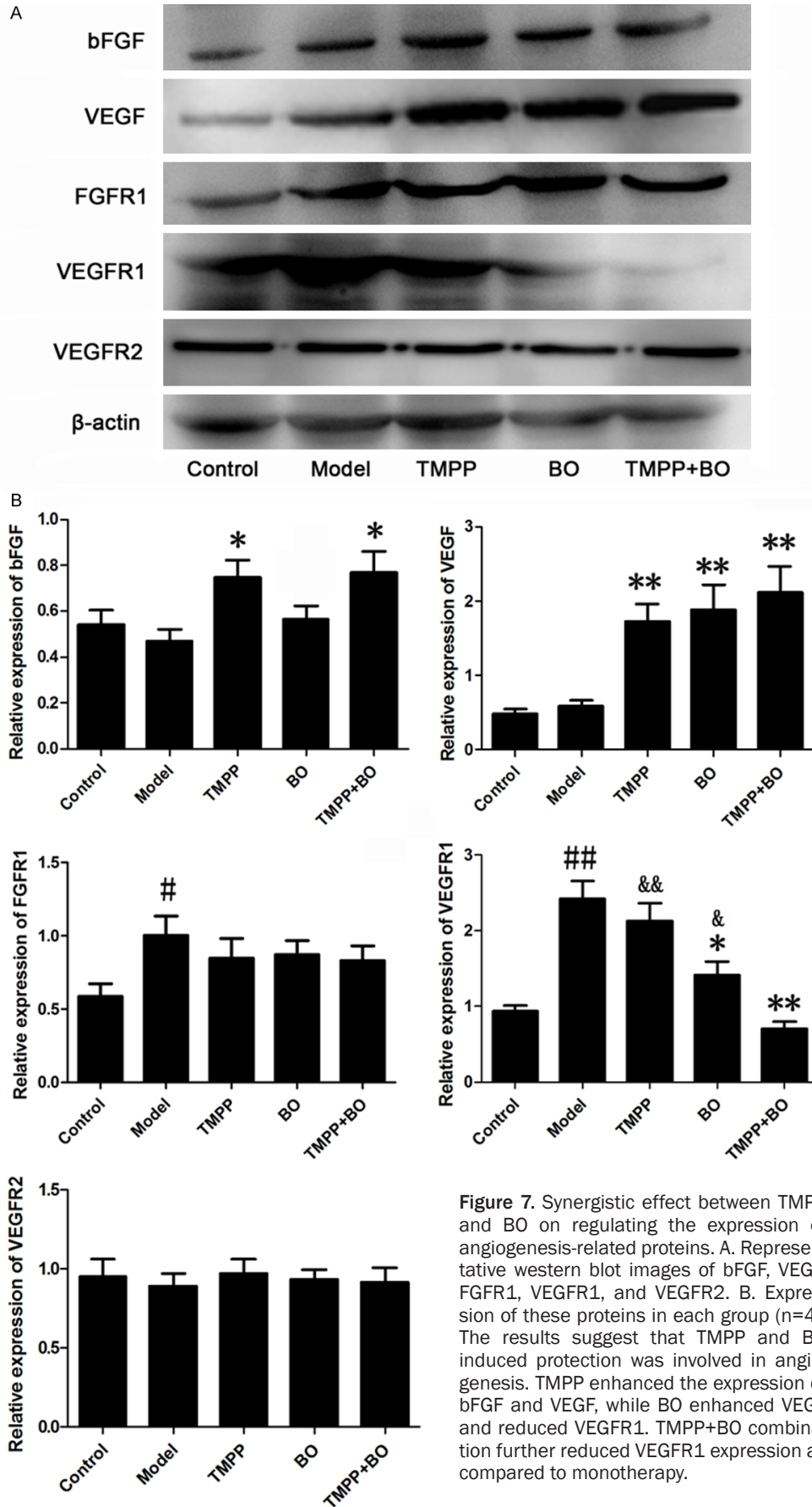
Figure 7. Synergistic effect between TMPP and BO on regulating the expression of angiogenesis-related proteins. A. Representative western blot images of bFGF, VEGF, FGFR1, VEGFR1, and VEGFR2. B. Expression of these proteins in each group (n=4). The results suggest that TMPP and BO induced protection was involved in angiogenesis. TMPP enhanced the expression of bFGF and VEGF, while BO enhanced VEGF and reduced VEGFR1. TMPP+BO combination further reduced VEGFR1 expression as compared to monotherapy.

purified caspase-3 accelerates apoptosis [28]. Therefore, caspase-3 has been referred to as the "death protein" [29]. Thus, the level of caspase-3 is a marker of apoptosis [30]. The bcl-2 family also regulates apoptosis, with the BAX/Bcl-2 ratio regarded as a switch to determine cell susceptibility to apoptosis [31]. Increasing evidence indicates that the p53 gene modulates apoptosis in response to hypoxia. p53 transcribes the pro-apoptotic BAX gene and induces caspase-3 activation and cellular death. Interestingly, in the present study, the Hoechst 33342 staining results were similar to flow cytometry. These results demonstrate that both TMPP and BO reduce apoptosis, and that their combination exhibits a synergistic effect with greater improvement than monotherapy. TMPP+BO showed synergistic protection against apoptosis in OGD-injured BMECs. Mechanistic studies verified that BO increases the expression of BCL-2 and decreases BAX. BCL-2 BAX Additionally, TMPP and TMPP+BO reduced the levels of p53 and caspase-3, two genes closely related to apoptosis. Compared to the TMPP group, the combination group exhibited a stronger modulation of BCL-2 and BAX. While compared to the BO group, the combination group displayed stronger modulation on the expression of all four genes. Modulation of apoptosis-related genes is in line with our results from the Hoechst 33342 staining and flow cytometry.

It was well known that angiogenic factors, such as bFGF, VEGF, and their receptors, play key roles in angiogenesis. bFGF was used to treat stroke up until 1999. Injection of bFGF decreased infarct volume in the ischemic penumbra during prolonged recovery [32]. Subsequently, others have reported that intravenous administration of bFGF in adult rats with cerebral ischemia induces cell proliferation and improves functional test results [33]. Furthermore, it was suggested that bFGF might stimulate downstream signaling pathways and regulate angiogenesis via its interaction with FGFR1 [34]. Under physiological conditions, endothelial cells express approximately 10 times less VEGFR1 than VEGFR2 [35]. Binding of VEGF to VEGFR2 activates intracellular tyrosine kinases and multiple downstream signals that induce angiogenesis. It was reported that inhibition of VEGFR2 signaling disturbs endothelial cell proliferation after stroke [36]. Subsequently, it was confirmed that VEGFR1, unlike activated VEG-

FR2, negatively regulates cell proliferation and reduces angiogenesis [37]. Increasing evidence suggests that cerebral ischemia upregulates VEGFR1 expression, which positively correlates to the degree of damage [38, 39], just as we observed in the present study. In the current study, we demonstrated that TMPP enhanced the expression of bFGF and VEGF, while BO elevated VEGF and reduced VEGFR1. TMPP+BO combination displayed significant modulation of bFGF, VEGF, and VEGFR1. Moreover, TMPP+BO combination had a stronger effect on angiogenesis than TMPP or BO monotherapy.

Conclusion

The present study demonstrates the synergistic effects of TMPP and BO in treating BMECs injured by OGD. Potential mechanisms involved were anti-oxidation, attenuation of Ca^{2+} overload, inhibition of apoptosis, and promotion of angiogenesis. Moreover, their synergistic effect was mainly related to the regulation of apoptosis and angiogenesis.

Acknowledgements

Disclosure of conflict of interest

None.

Address correspondence to: Ming Ruan, Jiangsu Key Laboratory for Pharmacology and Safety Evaluation of Chinese Materia Medica, School of Pharmacy, Nanjing University of Chinese Medicine, Nanjing 210023, China. E-mail: 1169195814@qq.com; Xiang-Chun Shen, The Key Laboratory of Optimal Utilization of Natural Medicinal Resources, Guizhou

Medical University, Huaxi College Station, Guian New District, Guiyang 550025, China. E-mail: shenxiangchun@126.com

References

[1] Navarro-Sobrino M, Rosell A, Hernandez-Guillamon M, Penalba A, Ribo M, Alvarez-Sabin J and Montaner J. Mobilization, endothelial differentiation and functional capacity of endothelial progenitor cells after ischemic stroke. Microvasc Res 2010; 80: 317-323.

[2] Yang H, Xi X, Zhao B, Su Z and Wang Z. KLF4 protects brain microvascular endothelial cells from ischemic stroke induced apoptosis by transcriptionally activating MALAT1. Biochem Biophys Res Commun 2018; 495: 2376-2382.

[3] Wang GF, Shi CG, Sun MZ, Wang L, Wu SX, Wang HF, Xu ZQ and Chen DM. Tetramethylpyrazine attenuates atherosclerosis development and protects endothelial cells from ox-LDL. Cardiovasc Drugs Ther 2013; 27: 199-210.

[4] Yang C, Xu Y, Zhou H, Yang L, Yu S, Gao Y, Huang Y, Lu L and Liang X. Tetramethylpyrazine protects CoCl2-induced apoptosis in human umbilical vein endothelial cells by regulating the PHD2/HIF/1alpha-VEGF pathway. Mol Med Rep 2016; 13: 1287-1296.

[5] Zhang M, Gao F, Teng F and Zhang C. Tetramethylpyrazine promotes the proliferation and migration of brain endothelial cells. Mol Med Rep 2014; 10: 29-32.

[6] Chen XH, Lin ZZ, Liu AM, Ye JT, Luo Y, Luo YY, Mao XX, Liu PQ and Pi RB. The orally combined neuroprotective effects of sodium ferulate and borneol against transient global ischaemia in C57 BL/6J mice. J Pharm Pharmacol 2010; 62: 915-923.

[7] Kong QX, Wu ZY, Chu X, Liang RQ, Xia M and Li L. Study on the anti-cerebral ischemia effect of borneol and its mechanism. Afr J Tradit Complement Altern Med 2014; 11: 161-164.

[8] Liu R, Zhang L, Lan X, Li L, Zhang TT, Sun JH and Du GH. Protection by borneol on cortical neurons against oxygen-glucose deprivation/reperfusion: involvement of anti-oxidation and anti-inflammation through nuclear transcription factor kappaappaB signaling pathway. Neuroscience 2011; 176: 408-419.

[9] Dong T, Chen N, Ma X, Wang J, Wen J, Xie Q and Ma R. The protective roles of L-borneolum, D-borneolum and synthetic borneol in cerebral ischaemia via modulation of the neurovascular unit. Biomed Pharmacother 2018; 102: 874-883.

[10] Yu B, Ruan M, Cui XB, Guo JM, Xu L and Dong XP. Effects of borneol on the pharmacokinetics of geniposide in cortex, hippocampus, hypothalamus and striatum of conscious rat by si-

[11] Yu B, Ruan M, Sun Y, Cui X, Yu Y, Wang L and Fang T. Effect of borneol and electroacupuncture on the distribution of hyperforin in the rat brain. Neural Regeneration Research 2011; 6: 1876-1882.

[12] Zheng Q, Chen ZX, Xu MB, Zhou XL, Huang YY, Zheng GQ and Wang Y. Borneol, a messenger agent, improves central nervous system drug delivery through enhancing blood-brain barrier permeability: a preclinical systematic review and meta-analysis. Drug Deliv 2018; 25: 1617-1633.

[13] Wu JY, Li YJ, Yang L, Hu YY, Hu XB, Tang TT, Wang JM, Liu XY and Xiang DX. Borneol and Alpha-asarone as adjuvant agents for improving blood-brain barrier permeability of puerarin and tetramethylpyrazine by activating adenosine receptors. Drug Deliv 2018; 25: 1858-1864.

[14] Yu B, Ruan M, Zhang ZN, Cheng HB and Shen XC. Synergic effect of borneol and ligustrazine on the neuroprotection in global cerebral ischemia/reperfusion injury: a region-specificity study. Evid Based Complement Alternat Med 2016; 2016: 4072809.

[15] Yu B, Ruan M, Liang T, Huang SW, Yu Y, Cheng HB and Shen XC. The synergic effect of tetramethylpyrazine phosphate and borneol for protecting against ischemia injury in cortex and hippocampus regions by modulating apoptosis and autophagy. J Mol Neurosci 2017; 63: 70-83.

[16] Yu B, Ruan M, Liang T, Huang SW, Liu SJ, Cheng HB and Shen XC. Tetramethylpyrazine phosphate and borneol combination therapy synergistically attenuated ischemia-reperfusion injury of the hypothalamus and striatum via regulation of apoptosis and autophagy in a rat model. Am J Transl Res 2017; 9: 4807-4820.

[17] Wu KW, Kou ZW, Mo JL, Deng XX and Sun FY. Neurovascular coupling protects neurons against hypoxic injury via inhibition of potassium currents by generation of nitric oxide in direct neuron and endothelium cocultures. Neuroscience 2016; 334: 275-282.

[18] Wu KW, Lv LL, Lei Y, Qian C and Sun FY. Endothelial cells promote excitatory synaptogenesis and improve ischemia-induced motor deficits in neonatal mice. Neurobiol Dis 2019; 121: 230-239.

[19] Lathey JL, Wiley CA, Verity MA and Nelson JA. Cultured human brain capillary endothelial cells are permissive for infection by human cytomegalovirus. Virology 1990; 176: 266-273.

[20] Bocci G, Fasciani A, Danesi R, Viacava P, Genazzani AR and Del Tacca M. In-vitro evidence of autocrine secretion of vascular endo-

thelial growth factor by endothelial cells from human placental blood vessels. Mol Hum Reprod 2001; 7: 771-777.

[21] Wang J, Li PT, Du H, Hou JC, Li WH, Pan YS and Chen HC. Tong Luo Jiu Nao injection, a traditional Chinese medicinal preparation, inhibits MIP-1beta expression in brain microvascular endothelial cells injured by oxygen-glucose deprivation. J Ethnopharmacol 2012; 141: 151-157.

[22] Wang W, Jiang B, Sun H, Ru X, Sun D, Wang L, Wang L, Jiang Y, Li Y, Wang Y, Chen Z, Wu S, Zhang Y, Wang D, Wang Y, Feigin VL; NESS-China Investigators. Prevalence, incidence, and mortality of stroke in China: results from a nationwide population-based survey of 480 687 adults. Circulation 2017; 135: 759-771.

[23] Chen ZZ, Yang DD, Zhao Z, Yan H, Ji J and Sun XL. Memantine mediates neuroprotection via regulating neurovascular unit in a mouse model of focal cerebral ischemia. Life Sci 2016; 150: 8-14.

[24] Birmingham K. Future of neuroprotective drugs in doubt. Nat Med 2002; 8: 5.

[25] Jensen RV, Andreadou I, Hausenloy DJ and Botker HE. The role of O-GlcNAcylation for protection against ischemia-reperfusion injury. Int J Mol Sci 2019; 20.

[26] Mishra V, Verma R and Raghubir R. Neuroprotective effect of flurbiprofen in focal cerebral ischemia: the possible role of ASIC1a. Neuropharmacology 2010; 59: 582-588.

[27] Dhar-Mascareno M, Carcamo JM and Golde DW. Hypoxia-reoxygenation-induced mitochondrial damage and apoptosis in human endothelial cells are inhibited by vitamin C. Free Radic Biol Med 2005; 38: 1311-1322.

[28] Teschendorf P, Vogel P, Wippel A, Krumnikl JJ, Spohr F, Bottiger BW and Popp E. The effect of intracerebroventricular application of the caspase-3 inhibitor zDEVD-FMK on neurological outcome and neuronal cell death after global cerebral ischaemia due to cardiac arrest in rats. Resuscitation 2008; 78: 85-91.

[29] Bell JD. Molecular cross talk in traumatic brain injury. J Neurosci 2007; 27: 2153-2154.

[30] Zhang Y, Lan R, Wang J, Li XY, Zhu DN, Ma YZ, Wu JT and Liu ZH. Acupuncture reduced apoptosis and up-regulated BDNF and GDNF expression in hippocampus following hypoxia-ischemia in neonatal rats. J Ethnopharmacol 2015; 172: 124-132.

[31] Wang GH, Lan R, Zhen XD, Zhang W, Xiang J and Cai DF. An-Gong-Niu-Huang Wan protects against cerebral ischemia induced apoptosis in rats: up-regulation of Bcl-2 and down-regulation of Bax and caspase-3. J Ethnopharmacol 2014; 154: 156-162.

[32] Ay H, Ay I, Koroshetz WJ and Finklestein SP. Potential usefulness of basic fibroblast growth factor as a treatment for stroke. Cerebrovasc Dis 1999; 9: 131-135.

[33] Wang ZL, Cheng SM, Ma MM, Ma YP, Yang JP, Xu GL and Liu XF. Intranasally delivered bFGF enhances neurogenesis in adult rats following cerebral ischemia. Neurosci Lett 2008; 446: 30-35.

[34] Pang Q, Zhang H, Chen Z, Wu Y, Bai M, Liu Y, Zhao Y, Tu F, Liu C and Chen X. Role of caveolin-1/vascular endothelial growth factor pathway in basic fibroblast growth factor-induced angiogenesis and neurogenesis after treadmill training following focal cerebral ischemia in rats. Brain Res 2017; 1663: 9-19.

[35] De Val S and Black BL. Transcriptional control of endothelial cell development. Dev Cell 2009; 16: 180-195.

[36] Shimotake J, Derugin N, Wendland M, Vexler ZS and Ferriero DM. Vascular endothelial growth factor receptor-2 inhibition promotes cell death and limits endothelial cell proliferation in a neonatal rodent model of stroke. Stroke 2010; 41: 343-349.

[37] Mendes RT, Nguyen D, Stephens D, Pamuk F, Fernandes D, Hasturk H, Van Dyke TE and Kantarci A. Hypoxia-induced endothelial cell responses - possible roles during periodontal disease. Clin Exp Dent Res 2018; 4: 241-248.

[38] Causey MW, Salgar S, Singh N, Martin M and Stallings JD. Valproic acid reversed pathologic endothelial cell gene expression profile associated with ischemia-reperfusion injury in a swine hemorrhagic shock model. J Vasc Surg 2012; 55: 1096-1103, e1051.

[39] Yoo KY, Hwang IK, Lee CH, Choi JH, Kwon SH, Kang IJ, You SG, Kim YM and Won MH. Difference of fibroblast growth factor receptor 1 expression among CA1-3 regions of the gerbil hippocampus after transient cerebral ischemia. J Neurol Sci 2010; 296: 13-21.